HTML ABSTRACT + LINKS

NiGe on Ge(001) by reactive deposition epitaxy: An *in situ* ultrahigh-vacuum transmission-electron microscopy study

R. Nath, C. W. Soo, C. B. Boothroyd, M. Yeadon, and D. Z. Chi
Institute of Materials Research and Engineering, 3 Research Link, Singapore S117602, Singapore

H. P. Sun, Y. B. Chen, and X. Q. Pan
Department of Materials Science and Engineering, University of Michigan, Ann Arbor, Michigan 48109-2136

Y. L. Foo[a)]
Institute of Materials Research and Engineering, 3 Research Link, Singapore S117602, Singapore

(Received 14 January 2005; accepted 1 April 2005; published online 12 May 2005)

We use an ultrahigh-vacuum transmission-electron microscopy, equipped with an electron-beam evaporator directed at a heating stage in the pole piece, to follow the reaction pathway of Ni on Ge(001) substrate at 300 °C. Using reactive deposition, we illustrate that epitaxial orthorhombic NiGe ($a=5.381$ Å, $b=3.428$ Å, and $c=5.811$ Å) phase can be grown directly without the initial formation of metal-rich Ni_2Ge phase. The epitaxial orientation of the NiGe islands and the underlying Ge(001) substrate were found to be NiGe($\bar{1}01$)//Ge(001) and NiGe[010]//Ge[110].
© *2005 American Institute of Physics*. [DOI: 10.1063/1.1929100]

Transition metal germanides are of intense engineering interest in nano/microelectronics and optoelectronics because of their potential as ohmic contacts in generation devices based on $Si_{1-x}Ge_x$ and Ge layers (ITRS 2003). One of the most important approaches in enhancing device speed is based on high performance substrate layers,[1–4] for example, $Si_{1-x}Ge_x$ and Ge-on-insulator (GOI). With the confluence in rapid development of high-k dielectrics, device technology based on these substrates is becoming a reality in manufacturing.[5] The use of SiGe and Ge substrates, introduced or to be introduced to enhance the carrier mobility and thereby further increase the device switching speed, will necessitate the switch from NiSi, a new silicide material to be introduced at sub-90-nm-technology nodes to replace conventional $CoSi_2$ in Si substrate technology, to NiSi(Ge) and/or Ni(Ge)—one of the most likely germanides for use as contact material in Ge-based complementary metal oxide semiconductor.

While numerous work has been reported on silicides (e.g., Ti, Co, Ni, Pt, Er, and Pd)[6–11] there is very little corresponding literature on germanides, a potentially important class of contact metallurgy for Ge/SiGe based devices. For contact applications in nanoscale electronics, epitaxial growth is preferred as it reduces interface roughness. We have recently investigated the epitaxial growth of Co on Ge(001) by reactive deposition epitaxy (RDE) at 350 °C where we observed the Co_5Ge_7 phase forming with an orientation relation defined by $Co_5Ge_7(001)\langle 110\rangle//Ge(001)\times\langle 100\rangle$ and $Co_5Ge_7(110)\langle 001\rangle//Ge(001)\langle 100\rangle$.[12] Another metal of interest in germanide formation is Ni. The Ni–Ge phase diagram is complex, with several invariant reactions and its thin film formation/reaction pathway is not generally considered well understood. While the more common Ni phases, i.e., Ni_3Ge, Ni_5Ge_2, Ni_5Ge_3, Ni_2Ge, and NiGe are more established in the literature, other phases such as $Ni_{19}Ge_{12}$, have only been reported by Ellner *et al.*[13] Polycrystalline Ni_2Ge and NiGe were formed during annealing of 1000–1500 Å thick Ni films on Ge(001) at temperatures from 150 to 600 °C (Ref. 14) with the first phase formed, as predicted by the rule of Walser and Bené,[15] being Ni_2Ge. Partial epitaxial growth of Ni_2Ge and NiGe was also reported on Ge(111) at annealing temperatures of 160 and 250 °C, respectively.[16]

In this letter, we report the epitaxial growth of NiGe on Ge(001) using RDE at 300 °C in an *in situ* ultrahigh vacuum transmission electron microscope (UHV-TEM). We observed epitaxial NiGe nucleation, island growth, and coalescence on Ge(001) substrates.

The reactive deposition of Ni on Ge(001) was carried in the pole piece of a modified TEM that enables us to monitor the growth and microstructural evolution *in situ*. The system (JEOL JEM-2000V), with a base pressure of 1×10^{-9} Torr (see Ref. 17), is equipped with an electron beam evaporator (Ni rod, 99.999%), sample heating capability (room temperature to 1200 °C), a Gatan Image Filter (GIF) and a Gatan Dual-Vision (DV) digital camera. To prepare a Ge substrate for deposition, a sample of dimensions 2.5×2.5 mm was cut from a Ge(001) wafer with resistivity 17–35 Ω cm. The Ge(001) substrate was mechanically polished and Ar^+ ion milled from the backside to obtain an electron transparent Ge specimen. This Ge(001) specimen was cleaned in deionized H_2O to remove oxide and mounted on a 6.5×2 mm Si(001) plate (*p*-type, resistivity 6–9 Ω cm), which acted as a heating medium to allow resistive heating of the Ge substrates.

The samples were degassed at ~250 °C for 2 h and then flashed *in situ* to remove native oxide, before being cooled to room temperature. The absence of oxide and carbon contaminants was confirmed from electron diffraction and electron energy loss spectroscopy (EELS). The Ge(001) substrate was then heated to 300 °C, the desired temperature for the reactive deposition experiment. The Ni deposition was carried out by *in situ* electron beam evaporation at a rate of ~80 Å per hour. The Ni flux was calibrated by Rutherford

a)Author to whom correspondence should be addressed; electronic mail: yl-foo@imre.a-star.edu.sg

 © 2005 American Institute of Physics
Downloaded 31 May 2005 to 202.6.242.69. Redistribution subject to AIP license or copyright, see http://apl.aip.org/apl/copyright.jsp

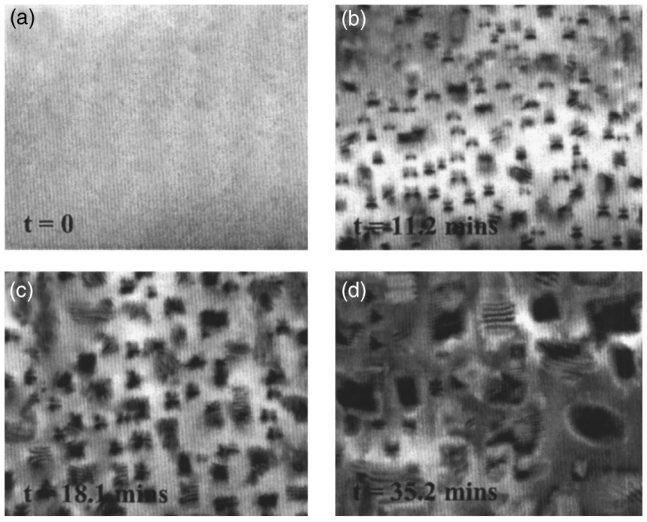

FIG. 1. Bright-field images of the Ge(001) surface during deposition of Ni: (a) Clean Ge(001) surface before deposition; NiGe on Ge(001) after deposition times of (b) t=11.2 min; (c) t=18.1 min, and (d) t=35.2 min.

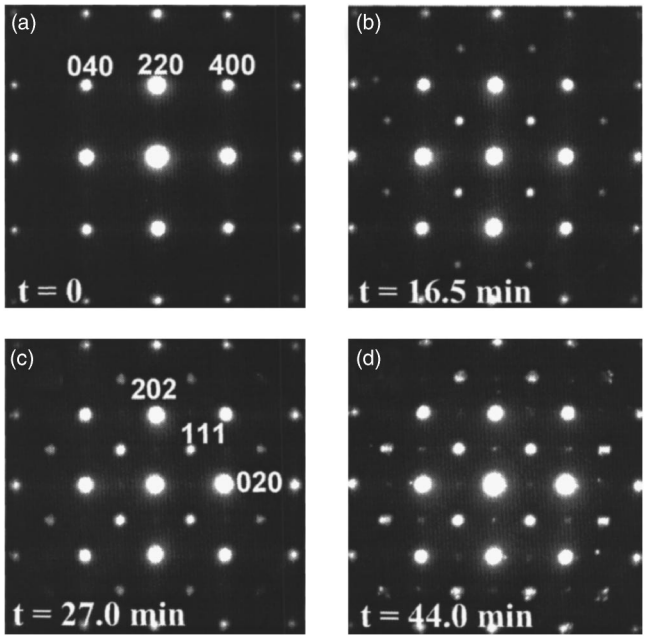

FIG. 2. (a) Diffraction pattern from the clean Ge(001) surface before deposition of Ni. Diffraction patterns from NiGe on Ge(001) after deposition times of (b) t=16.5 min, (c) t=27.0 min, and (d) t=44.0 min.

backscattering spectroscopy and cross-sectional transmission electron microscopy. The total deposition time was 45 min. Real-time data acquisition during growth for both images and electron diffraction patterns during deposition was carried out using the Gatan DV digital camera.

The epitaxial growth of the orthorhombic NiGe phase during RDE at 300 °C is shown the series of bright-field TEM images in Fig. 1. The bright-field image of the Ge(001) substrate prior to deposition, as shown in Fig. 1(a), is essentially featureless. When the shutter is opened, we observed spatially random islands nucleating on the Ge(001) surface. In a bright-field image, the nucleating NiGe islands appear darker in contrast due to their diffraction contrast. The number density of such islands (n) increased rapidly, in the classical nucleation regime, before reaching a steady state at $t \sim 6.5$ min. As the islands grew in size, moiré fringes due to the lattice mismatch between the nucleating phase and the Ge(001) substrate were observed. The very initial moiré fringes appeared as two dots, followed by four dots in a butterfly shape before they joined together to form a series of band-like fringes. These moiré fringes are well-aligned perpendicular to either the [010] or [100] azimuth of the Ge(001) substrate. The average spacing of the fringes is 55 Å. An example is shown in Fig. 1(b) at $t=11.2$ min, at an equivalent Ni deposition thickness of 25 Å. Further deposition resulted in island growth of the NiGe as shown in Fig. 1(c), at $t=18.1$ min, where the lateral dimension of the islands grows. After 35.2 min of deposition, the islands coalesced, as shown in Fig. 1(d).

The structural evolution of the orthorhombic NiGe islands can be determined from diffraction patterns taken as a function of deposition time. The diffraction pattern of the clean Ge(001) substrate prior to deposition as shown in Fig. 2(a) consists of 220 and 400 Ge spots, without diffuse scattering or a ring pattern, indicating that the initial substrate is highly crystalline and clean. This is consistent with the EELS spectra taken prior to deposition, which show the absence of C and O. Upon deposition, we observed new sets of diffraction spots appearing, which increase in intensity with deposition time. The new diffraction spots appear in the Ge 200 positions [see Fig. 2(b)] and their intensity is symmetrical about the central spot, establishing that the island growth observed in the series of bright-field images in Figs. 1(b)–1(d) is epitaxial to the substrate. Further deposition leads to the appearance of a second set of diffraction spots of lower intensity at the Ge 110 positions. An example is shown in Fig. 2(c) at $t=27$ min. These observations are consistent with orthorhombic NiGe ($a=5.381$ Å, $b=3.428$ Å, $c=5.811$ Å; JCPDS-ICDD PDF No. 07-0297) having an orientation relation $\mathrm{NiGe}(\bar{1}01)//\mathrm{Ge}(001)$ and $\mathrm{NiGe}[010]//\mathrm{Ge}[110]$.[18] The spots at the Ge 200 positions are from NiGe 111.

At $t>23.2$ min the diffraction behavior becomes less clear. The NiGe 202 spot ($d_{202}=1.97$ Å) still lie on top of the Ge 220 spots ($d_{220}=2.00$ Å) as expected from their similar spacing. The NiGe 020 spots are now visible just outside the Ge 220 spots [Fig. 2(d)] but their measured spacing is 1.92 Å, somewhat larger than the spacing for bulk NiGe of 1.72 Å. This suggests that there is still considerable strain present even after 23 min of deposition. The strain can also be deduced from the moiré fringes visible in Figs. 1(c) and 1(d). For unstrained crystals the moiré fringes would be parallel to the sides of the particles and of similar spacing. However, in both Figs. 1(c) and 1(d) many moiré fringe spacings are visible and the moiré fringes are bent, indicating strain within the crystals.

Ideally, for device processing especially in nanoscale electronics, the first phase to form for metal contact should also be the final phase because reorientation of nonepitaxial phases formed at lower temperatures by a mechanism such as grain growth is unlikely once such regions have nucleated. In addition, the germanide phase formed should be epitaxial[19] as this reduces interface roughness that may puncture ultrashallow p-n junctions. The well-known Walser and Bené (WB) postulate proposes that the first crystalline phase nucleated will be the congruently melting phase next to the lowest temperature eutectic in a binary couple. Based on Ni–Ge phase diagram,[20] the WB rule indicates that metal-

Downloaded 31 May 2005 to 202.6.242.69. Redistribution subject to AIP license or copyright, see http://apl.aip.org/apl/copyright.jsp

rich Ni_2Ge phase will form first if we anneal a Ni–Ge interface at subeutectic temperature, in agreement with Wittmer *et al.*[14] In their experiment, upon annealing at the higher temperature of 250 °C, Ni_2Ge reacts to form the mono Ni germanide. However, in the Wittmer *et al.* study using x-ray diffraction, there was no report of the initial crystallographic orientation of Ni_2Ge or whether there is a reorientation of subsequent NiGe phase with respect to the underlying Ge(001) substrate, which is crucial information for engineering applications in submicron devices.

We used UHV-TEM as a tool in developing insights of reaction pathway of Ni on Ge(001). In order to circumvent the formation of the low-temperature Ni_2Ge phase as predicted by WB, we used reactive deposition at 300 °C in an attempt to directly deposit epitaxial NiGe phase without formation of intervening Ni_2Ge phase. In this letter we illustrated that by using reactive deposition, we can grow orthorhombic NiGe phase that is stable up to 600 °C—well within the thermal budget for device processing, epitaxially on Ge(001). Since the key parameter in the experiment is deposition temperature, we expect the RDE technique of Ni deposition at elevated Ge substrate temperature ($\sim$300 °C) may be applied to any other thin film deposition techniques such as sputtering—a widely used industrial process, to directly deposit the NiGe phase on Ge(001) in nano/microelectronics processing industry.

In summary we used *in situ* UHV-TEM to follow the reaction pathway during Ni deposition on Ge(001) at 300 °C. Using RDE, we avoid the formation of the lower-temperature Ni rich Ni_2Ge phase. The NiGe phase was formed with an orientation relation to the substrate given by $NiGe(\bar{1}01)//Ge(001)$ and $NiGe[010]//Ge[110]$. By using the inherent capability of TEM in structure analysis and imaging, we have captured in real time, epitaxial NiGe island nucleation, growth, and coalescence through diffraction patterns and bright-field imaging at nanometer resolution.

The authors acknowledge the financial support of the Institute of Materials Research and Engineering (IMRE) and the Department of Materials Science (DMS) at the National University of Singapore (NUS). H.P.S., Y.B.C., and X.Q.P. acknowledge support of the NSF through Grant No. NSF/DMR 0308012. Y.L.F. also acknowledges useful discussion with Dr. Eng-Soon Tok of DMS at NUS.

[1] M. L. Lee and E. A. Fitzgerald, *IEEE International Electron Devices Meeting*, 18.1.1 (2003).
[2] C. W. Leitz, M. T. Currie, M. L. Lee, Z. Y. Cheng, D. A. Antoniadis, and E. A. Fitzgerald, J. Appl. Phys. **92**, 3745 (2002).
[3] M. L. Lee, C. W. Leitz, Z. Y. Cheng, A. J. Pitera, T. A. Langdo, M. T. Currie, G. Taraschi, E. A. Fitzgerald, and D. A. Antoniadis, Appl. Phys. Lett. **79**, 3344 (2001).
[4] *Properties of Silicon Germanium and SiGe:Carbon*, edited by E. Kasper, and K. Lyutovich (The Institution of Electrical Engineers, London, 2000).
[5] O. Sneh, R. B. Clark-Phelps, A. R. Londergan, J. Winkler, and T. E. Seidel, Thin Solid Films **402**, 248 (2002).
[6] S. L. Zhang, C. Lavoie, C. Cabral, J. M. E. Harper, F. M. d'Heurle, and J. Jordan-Sweet, J. Appl. Phys. **85**, 2617 (1999).
[7] M. L. A. Dass, D. B. Fraser, and C. S. Wei, Appl. Phys. Lett. **58**, 1308 (1991).
[8] D. Mangelinck, J. Y. Dai, J. S. Pan, and S. K. Lahiri, Appl. Phys. Lett. **75**, 1736 (1999).
[9] N. Franco, J. E. Klepeis, C. Bostedt, T. Van Buuren, C. Heske, O. Pankratov, T. A. Callcott, D. L. Ederer, and L. J. Terminello, Phys. Rev. B **68**, 045116 (2003).
[10] G. Chen, J. Wan, J. S. Yang, X. M. Ding, L. Ye, and X. Wang, Surf. Sci. **513**, 203 (2002).
[11] P. Gergaud, M. Megdiche, O. Thomas, and B. Chenevier, Appl. Phys. Lett. **83**, 1334 (2003).
[12] H. P. Sun, Y. B. Chen, X. Q. Pan, D. Z. Chi, R. Nath, and Y. L. Foo, Appl. Phys. Lett. **86**, 071904 (2005).
[13] M. Ellner, T. Goedecke, and K. Schubert, J. Less-Common Met. **24**, 23 (1971).
[14] M. Wittmer, M.-A. Nicolet, and J. W. Mayer, Thin Solid Films **42**, 51 (1976).
[15] R. M. Walser and R. W. Bené, Appl. Phys. Lett. **28**, 624 (1976).
[16] Y. F. Hsieh, L. J. Chen, E. D. Marshall, and S. S. Lau, Thin Solid Films **162**, 287 (1988).
[17] R. K. K. Chong, M. Yeadon, W. K. Choi, E. A. Stach, and C. B. Boothroyd, Appl. Phys. Lett. **82**, 1833 (2003).
[18] W. B. Pearson, *Pearson's Handbook of Crystallographic Data for Intermetallic Phase* (ASM, Metals Park, OH, 1997).
[19] R. T. Tung, Mater. Chem. Phys. **32**, 107 (1992).
[20] *Phase Diagrams of Binary Nickel Alloys*, edited by P. Nash (ASM, Metals Park, OH, 1991).

Downloaded 31 May 2005 to 202.6.242.69. Redistribution subject to AIP license or copyright, see http://apl.aip.org/apl/copyright.jsp